

are produced naturally in the sample when a given minority site is surrounded by majority sites. In such a case the wave function can be confined by the surrounding solid and the vacuum barrier. In effect, an analog of a quantum dot is formed, which is smaller by at least two orders of magnitude than any quantum dot structure to date (1). However, unlike quantum dots, the discrete states formed are not the result of size quantization but are localized quasi-atomic states. An NDR site that shows a type b I - V curve (Fig. 2) is shown in Fig. 1b. NDR appears when the STM tip is over the bright inner core of this site. Thus, NDR is localized in a region of about 10 Å. On the basis of local-density-functional theory calculations (5), we tentatively identify this site as involving a missing Si adatom over a B_s site. In this way, a localized state involving three Si dangling bonds is formed. In other experiments we find type c I - V behavior over Si-T₄ sites. Such NDR behavior has also been observed recently by another group (11). Type d I - V behavior is observed over more complex, as yet unassigned sites.

Although localized states at the sample appear to be essential for the development of NDR, we have evidence that the tip electronic structure is equally important. In fact, we have observed rest-atom NDR over adatom sites of the clean Si(111) (7 × 7) surface after the tungsten tip became coated with Si by crashing into the Si sample. Because of the large separation between rest-atoms on the 7 × 7 surface, the Si adatom surface states are localized, as is evidenced by the lack of dispersion in angularly resolved photoemission (12). When atomic resolution is achieved by STM, it is expected that tunneling at the tip involves very few (for example, one to three) tip atoms on top of a macroscopic tip surface. Under these conditions we do not expect that the relevant tip states are extended states; most likely they can be described as adsorption-induced resonances with a Lorentzian-like density of states (DOS) (13). The width of such states depends on the number of atoms that are involved in the tunneling and their coupling to the rest of the tip. For example, if tunneling occurs out of an impurity atom that is relatively weakly coupled to the tip, the relevant tip DOS can be quite narrow. During an STM experiment, the structure of the active area of the tip and even the chemical nature of the tip atom directly involved in the tunneling can change as atoms move on the surface of the tip.

Using the idea that NDR arises as a result of tunneling between localized states, we have performed simulations of I - V characteristics for the sets of DOS for sample and tip shown in Fig. 3 (left) and a simple one-

dimensional model for the tunneling barrier. The DOS of the sample states were obtained through STM measurements with "normal" tips, that is, tips with which no NDR behavior is observed and which give tunneling spectra for the majority sites that are in agreement with conventional spectroscopy (14). The results are shown in Fig. 3 (right). When the bias voltage is varied, the peaks in DOS shift with respect to each other. When the peak positions coincide, the tunneling current exhibits a maximum in cases a and b. In case c, maxima are observed when the Fermi level crosses a peak in the DOS. Similar behavior was observed in a first-principles calculation by Lang (15). From Fig. 3 it is clear that by including sites with prominent localized occupied or unoccupied states, we can account for all observed I - V behaviors shown in Fig. 1. These results provide support for our proposal that the mechanism of NDR involves tunneling between localized atomic-like states.

Our results show that the property of NDR can be realized in the I - V characteristics of a diode formed by an STM tip and localized surface sites. In the future it may be possible to construct atomic scale devices that use the characteristics of atomic wave functions.

REFERENCES AND NOTES

1. H. Heinrich, G. Bauer, F. Kucher, Eds., *Physics and Technology of Submicron Structures* (Springer Series in Solid State Sciences, vol. 83, Springer-Verlag, Berlin, 1988).
2. L. Esaki, *Phys. Rev.* **109**, 603 (1958).
3. S. M. Sze, *The Physics of Semiconductor Devices* (Wiley-Interscience, New York, 1981).
4. G. Binnig and H. Rohrer, *Rev. Mod. Phys.* **57**, 615 (1987); C. F. Quate, *Phys. Today* **39**, 26 (August 1986); R. M. Tromp, R. J. Hamers, J. E. Demuth, *Science* **234**, 304 (1986); P. K. Hansma, V. B. Elings, O. Marti, C. E. Bracker, *ibid.* **242**, 209 (1988).
5. I.-W. Lyo, E. Kaxiras, Ph. Avouris, *Phys. Rev. Lett.*, in press.
6. Ph. Avouris and R. Wolkow, *Phys. Rev. B* **39**, 5091 (1989); R. Wolkow and Ph. Avouris, *Phys. Rev. Lett.* **60**, 1049 (1988).
7. H. Hirayama, T. Tatsumi, N. Aizaki, *Surface Sci.* **193**, L47 (1988).
8. V. V. Korobtsov, V. G. Lifshits, A. V. Zotov, *ibid.* **195**, 467 (1988).
9. R. J. Hamers and J. E. Demuth, *Phys. Rev. Lett.* **60**, 2527 (1988).
10. J. Nogami, S. Park, C. F. Quate, *Phys. Rev. B* **35**, 4137 (1987).
11. P. Bedrossian, D. M. Chen, K. Mortensen, J. A. Golovchenko, *Bull. Am. Phys. Soc.* **34**, 720 (1989).
12. R. I. G. Uhrberg, G. V. Hansson, J. M. Nicholls, P. E. S. Persson, *Phys. Rev. B* **31**, 3805 (1985).
13. N. D. Lang and A. R. Williams, *ibid.* **18**, 616 (1978).
14. E. Kaxiras, K. C. Pandey, F. J. Himpsel, R. M. Tromp, in preparation.
15. N. D. Lang, *Phys. Rev. B* **34**, 5747 (1986).
16. We acknowledge useful discussions with N. D. Lang.

15 May 1989; accepted 2 August 1989

Spontaneous Vesicle Formation in Aqueous Mixtures of Single-Tailed Surfactants

ERIC W. KALER,*† A. KAMALAKARA MURTHY,*
BEATRIZ E. RODRIGUEZ,* JOSEPH A. N. ZASADZINSKI

Spontaneous, single-walled, equilibrium vesicles can be prepared from aqueous mixtures of simple, commercially available, single-tailed cationic and anionic surfactants. Vesicle size, surface charge, or permeability can be readily adjusted by varying the ratio of anionic to cationic surfactant. Vesicle formation apparently results from the production of anion-cation surfactant pairs that then act as double-tailed zwitterionic surfactants. These vesicles are quite stable in comparison to conventional vesicles prepared by mechanical disruption of insoluble liquid crystalline dispersions.

VESICLES, WHICH ARE SINGLE-BILAYER shells 30 to 150 nm in diameter, are widely used as model membranes, capsules for agents in assays and drug delivery, microreactors for artificial photosynthesis (among other reactions), and substrates for a variety of enzymes and

proteins (1, 2). Although vesicles often form spontaneously in vivo, they have only rarely been observed to form in vitro without the input of considerable mechanical energy (such as sonication or pressure filtration) or elaborate chemical treatments (detergent dialysis or reverse-phase evaporation) (1-3). Vesicles formed in this way are metastable and eventually revert to multilamellar liquid-crystalline aggregates. This reversion is invariably accompanied by a release of the vesicle contents and the failure of the vesicle carriers. The lack of a simple and general method for producing spontaneous and stable vesicles has inhibited further progress in

E. W. Kaler, A. K. Murthy, B. E. Rodriguez, Department of Chemical Engineering, BF-10, University of Washington, Seattle, WA 98195.

J. A. N. Zasadzinski, Department of Chemical and Nuclear Engineering, University of California, Santa Barbara, CA 93106.

*Present address: Department of Chemical Engineering, University of Delaware, Newark, DE 19716.

†To whom correspondence should be addressed.

these areas. There have been reports of spontaneous vesicle formation in certain mixtures of short- and long-chain, double-tailed lecithins (3), in solutions of double-tailed surfactants with hydroxide and other more exotic counterions (4), and in some mixtures of single-tailed surfactants (5). Although these systems were an improvement over conventional sonicated vesicles, the relatively restricted chemical or physical properties of the vesicles or the limited availability of the surfactants were such that these methods were not widely exploited.

We report a general method for preparing spontaneous, equilibrium vesicles of controlled size, surface charge, or permeability from commercially available surfactants. Vesicles formed immediately upon combining aqueous mixtures of two commercially available, single-tailed surfactants with oppositely charged head groups. This phenomenon appears to be general and has been observed in a variety of surfactants (6). This method of vesicle preparation offers a remarkably simple way of tailoring vesicle properties and allows gentle and efficient encapsulation to take place without mechanical or chemical perturbations from the final vesicle composition or structure. The curvature of the mixed surfactant bilayers (which controls size and shape), the vesicle wall thickness (which controls permeability), and the sign and magnitude of the surface charge (which control vesicle interactions and stability against aggregation) can be determined by the relative amounts and the chain length of the individual, commercially available surfactants used. We present results for aqueous mixtures of cetyl trimethylammonium tosylate (CTAT) and sodium dodecylbenzene sulfonate (SDBS) (6). Vesicle formation is demonstrated by quasi-elastic light

scattering (QLS), freeze-fracture transmission electron microscopy (TEM), and glucose entrapment experiments. The vesicles prepared from these surfactants range from about 30 to 80 nm in radius (depending on surfactant ratio and total concentration), can be prepared to be either positively or negatively charged, efficiently encapsulate and retain glucose and other solutes, and remain stable for at least 1 year.

We prepared the samples by first making stock solutions of either SDBS or CTAT of known concentration in deionized water. Both stock solutions were equilibrated at the temperature of interest, and gentle mixing of the solutions resulted in the spontaneous formation of vesicles (Fig. 1). Except for gentle mixing, the solutions were not subjected to any type of mechanical agitation. When a sample in the two-phase region was prepared, phase separation was occasionally accelerated by centrifugation of the sample at 400g. We used high-performance liquid chromatography to determine the ratio of tosylate and dodecylbenzene ion concentrations, a sodium ion-specific electrode to determine $[\text{Na}^+]$, and Karl Fischer titration to determine the water concentration. The vesicles survived freeze-thaw cycles except when the freezing path allowed the formation of a 1:1 $\text{DBS}^-:\text{CTA}^+$ complex, which does not dissolve. There is no evidence of a (first-order) micelle-vesicle phase transition as either of the micellar phases on the surfactant-water edges of the triangle is titrated against a micellar solution of the other surfactant. If any micelle-vesicle two-phase region exists, it is vanishingly small.

A spectrometer of standard design (7) was used for the QLS measurements. Solutions for light scattering were gravity filtered through a 0.22- μm Millipore filter into the

Table 1. Sizes of CTAT-SDBS vesicles, as determined by QLS, as a function of composition. Percentages are by weight.

Water (%)	CTAT/SDBS	Radius (Å)
99.7	<i>One-phase region</i>	
	2/8	330
	3/7	340
	4/6	450
	5/5	720
	6/4	500
	7/3	570
99.0	8/2	610
	9/1	580
98.0	1/9	430
	3/7	350
97.0	2/8	300
	8/2	560
95.0	1/9	470
	3/7	540
93.0	<i>Two-phase region</i>	
	1/9	550
	1/9	720
91.0	1/9	830

scattering cell. All measurements were done at a scattering angle of 90° , and the intensity autocorrelation function was analyzed by the method of cumulants (8). Measurements were made of vesicles in both the CTAT-rich and the SDBS-rich one-phase regions (Table 1). Samples in the CTAT-rich regions were in general more turbid than those in the SDBS-rich region, a result consistent with the presence of larger vesicles. Apparent vesicle size increased as the water content decreased at a constant SDBS/CTAT ratio, although no accounting of the effect of interparticle interactions on apparent size was made. The average vesicle radius was between 30 and 80 nm, and there was substantial size polydispersity, as manifested by large values of the variance (between 0.1 and 0.2), which is related to the second cumulant. The vesicles are charged, with SDBS-rich vesicles migrating toward the anode of an electrophoresis cell and CTAT-rich vesicles moving toward the cathode. The vesicles reform after freeze-thaw cycles, and the average size and variance of the size distribution are unaltered.

Samples for trapping experiments were prepared as described above with the substitution of 0.3M glucose solution for water. Vesicles formed in the presence of glucose were equal in size to those formed in pure water. The glucose-containing vesicles (1.5 ml) were put into a dialysis bag (Spectrapor standard cellulose tubing) and dialyzed against 500 ml of isotonic salt (0.075M KCl and 0.075M NaCl). Four dialyzate changes (at 3-hour intervals) were sufficient to quantitatively remove the glucose from the exterior of the vesicles as determined by the

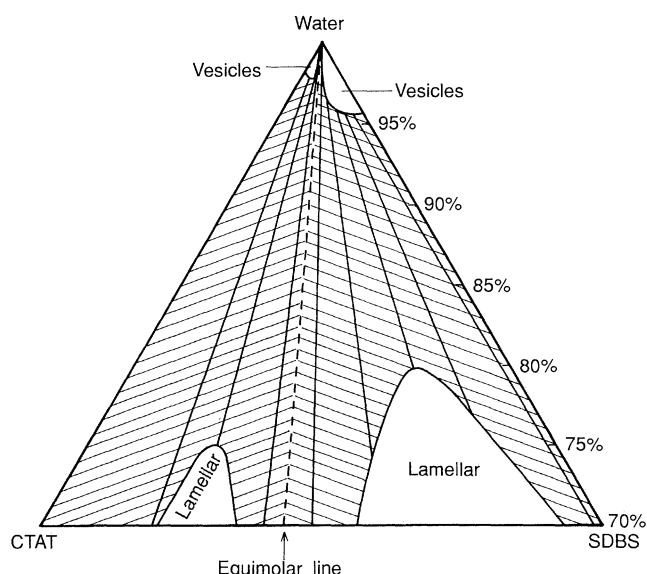


Fig. 1. CTAT-SDBS-water phase diagram at 25°C . The two one-phase regions in the water-rich corner contain vesicles. The two-phase region is cross-hatched, and the tie-lines have been determined experimentally.

change in absorbance at 340 nm due to the formation of the reduced form of nicotinamide adenine dinucleotide phosphate in the presence of glucose-6-phosphate dehydrogenase and hexokinase (9). Triton X-100 was then added to the sample in the dialysis bag to disrupt the vesicles and release the entrapped glucose. Disrupted vesicles were dialyzed for 3 hours, and assay of the dialyzed sample showed the presence of substantial glucose. There was some slight interference of the anionic surfactant with the kinetics of the enzymatic reaction.

We prepared samples for electron microscopy by sandwiching a thin layer (<50 μm) of the vesicle dispersion between two copper planchettes (RMC, Tucson, Arizona). We froze the sample sandwiches by placing them between opposed jets of liquid propane cooled by liquid nitrogen to -190°C in a Gilkey-Stachelin jet freeze device (RMC, Tucson, Arizona). The specimens were transferred under liquid nitrogen to a Reichert-Jung Cryofract 190 freeze-fracture device (Cambridge Instruments Inc., Buffalo, New York), fractured at -170°C and 10^{-9} torr, and immediately replicated with 1.0 nm of platinum-carbon alloy applied by electron-beam evaporation at 45° to the fracture surface, followed by the imposition of a 15-nm-thick reinforcing film of carbon, applied at normal incidence (10, 11). In the TEM images (JEOL 100 CX-II; 80 kV; initial magnification, $\times 40,000$) shadows appear light. We obtained vesicle size distributions by measuring the diameters of vesicles that showed well-defined shadows indicating that the fracture surface propagated near the center of the vesicle (12).

The CTAT-rich vesicle dispersion (Fig. 2A) showed a rather polydisperse size distribution with diameters ranging from about 10 nm to more than 250 nm (average diameter, about 70 nm). The vesicles were uniformly distributed throughout the sample, indicative of good freezing. No multilamellar vesicles were seen in this or in the SDBS-rich sample, although sometimes a small vesicle was embedded within a larger vesicle (Fig. 2A, bottom right). The size distribution of the SDBS-rich vesicle dispersion (Fig. 2B) sample was significantly narrower than that of the CTAT-rich dispersion, with an average diameter of about 60 nm. There appeared to be fewer large vesicles (>200-nm diameter) in the SDBS-rich dispersion than in the CTAT-rich dispersion. The number density of the SDBS vesicles appeared to be greater than in the CTAT-rich fraction, but this was not analyzed in detail.

The formation of equilibrium vesicles from mixtures of single-tailed surfactants is unexpected theoretically. Simple geometric

arguments (2) predict that amphiphiles with relatively large hydrophobic regions (tails) and relatively small hydrophilic head groups should form bilayer structures, as is observed, although spontaneous vesicle formation is rare (2-4). However, single-tailed amphiphiles with relatively small tail groups and large head groups are predicted to and invariably do form spherical or cylindrical micelles (2). Equimolar mixtures of anionic and cationic surfactants either form lamellar phase (13) or precipitate from solution. For these reasons, addition of a cationic surfactant to an anionic micellar solution is generally avoided in practice, and few examina-

tions of the phase diagrams have been made (14). Our experimental phase diagram bears a strong qualitative resemblance to that calculated by Jokela *et al.* (15), who used a cell model and assumed equilibria between lamellar (not vesicular) and crystalline phases in an anionic-cationic mixture. The two lamellar phases therein correspond to the vesicular phases in the water-rich corner of Fig. 1, and crystalline surfactant phases are predicted to be present in the surfactant-rich corners of the diagram.

Strong synergistic effects may occur in the surface activity of mixed surfactants (16-20), and ion-paired surfactants can be extremely surface-active. It is likely that the same mechanism is at work promoting vesicle formation; that is, anionic and cationic surfactants pair and form what is effectively a zwitterion at the vesicle surface. In this case, the ion pair has the geometric features of a small head group and large tail group thought necessary for vesicle formation. The residual unpaired surfactants help to fluidize the membrane and yield the net surface charge. Our results for the SDBS-CTAT solutions are representative for other mixtures. In each case, anionic surfactant-rich vesicles are charged negatively and the cationic-rich vesicles are charged positively. Vesicle radii appear to decrease as the tail lengths of the surfactants become more dissimilar.

These results illustrate a rich new area of surfactant phase behavior and suggest new formulations for stable vesicular structure that may be useful in addressing theoretical and practical problems. The generality of the results also indicates that mixed bilayers of appropriate biological surfactants can be tailored to have useful properties.

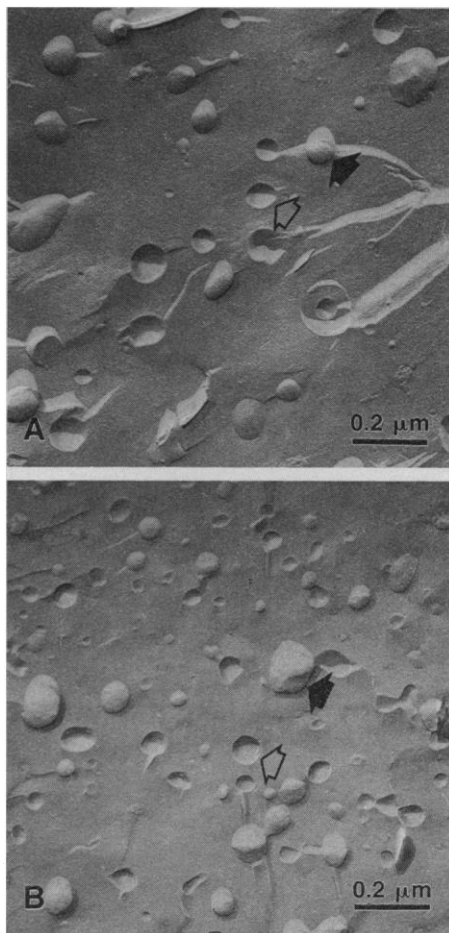


Fig. 2. (A) TEM image of a freeze-fractured CTAT-rich vesicle fraction (98% by weight water and CTAT/SDBS ratio of 4/1 by weight). The average vesicle diameter is 70 nm. The open arrow shows the shadow pattern of a vesicle plucked from the fracture surface, and the filled arrow shows the shadow pattern of a vesicle protruding from the surface. The vesicles are polydisperse, with diameters ranging from about 10 to about 250 nm. (B) TEM image of a freeze-fractured SDBS-rich vesicle fraction (98% by weight water and CTAT/SDBS ratio of 1/4 by weight). The average vesicle diameter is approximately 60 nm. Arrows are as in (A). The polydispersity in vesicle diameter is significantly less in the SDBS-rich vesicle fraction than in the CTAT-rich fraction, with fewer very large vesicles.

REFERENCES AND NOTES

1. J. Fendler, *Membrane Mimetic Chemistry* (Wiley, New York, 1983).
2. J. N. Israelachvili, *Intermolecular and Surface Forces* (Academic Press, Orlando, FL, 1985).
3. N. E. Gabriel and M. F. Roberts, *Biochemistry* **23**, 4011 (1984).
4. Y. Talmon, D. F. Evans, B. W. Ninham, *Science* **221**, 1047 (1983); J. E. Brady, D. F. Evans, B. Kachar, B. W. Ninham, *J. Am. Chem. Soc.* **106**, 4279 (1984).
5. W. R. Hargreaves and D. W. Deamer, *Biochemistry* **17**, 3759 (1978).
6. Spontaneous vesicle formation has also been observed in mixtures of the anionic surfactants dodecyl and octyl sodium sulfate and sodium benzene sulfonate (Tokyo Kasei, extra pure grade) with the cationic surfactants cetyltrimethylammonium tosylate (Alfa; recrystallized from *n*-propanol and ether) and cetyltrimethylammonium bromide.
7. N. J. Chang, thesis, University of Washington, Seattle (1986).
8. D. E. Koppel, *J. Chem. Phys.* **57**, 4814 (1972).
9. R. A. Demel, S. C. Kinsky, C. B. Kinsky, L. L. M. Van Deenen, *Biochim. Biophys. Acta* **150**, 665 (1968).
10. J. A. N. Zasadzinski and R. B. Meyer, *Phys. Rev.*

- Lett. 56, 636 (1986).
11. J. A. N. Zasadzinski, *J. Microsc. (Oxford)* 150, 137 (1988).
 12. R. van Venetië, J. Leunissen-Bijvelt, A. J. Verkleij, P. H. J. Th. Ververgaert, *ibid.* 118, 401 (1980).
 13. P. Jokela, B. Jonsson, A. Khan, *J. Phys. Chem.* 91, 3291 (1987).
 14. D. H. Chen and D. G. Hall, *Colloid Polym. Sci.* 251, 41 (1973); C. A. Barker, D. Saul, G. J. T. Tiddy, B. A. Wheeler, E. Willis, *J. Chem. Soc. Faraday Trans. 1* 70, 154 (1974); J. F. Scamehorn, Ed., *Phenomena in Mixed Surfactant Systems* (American Chemical Society, Washington, DC, 1986).
 15. P. Jokela, B. Jonsson, H. Wennerstrom, *Prog. Colloid Polym. Sci.* 70, 17 (1985).
 16. E. W. Anacker, *J. Colloid Interface Sci.* 8, 402 (1953).
 17. H. W. Hoyer, A. Marmo, M. Zoellner, *J. Phys. Chem.* 65, 1804 (1961).
 18. J. M. Corkill, J. F. Goodman, S. P. Harrold, J. R. Tate, *Trans. Faraday Soc.* 62, 994 (1966).
 19. D. Goralczyk, *J. Colloid Interface Sci.* 77, 68 (1980).
 20. E. H. Lucassen-Reynders, J. Lucassen, D. Gilles, *ibid.* 81, 150 (1981).
 21. Financial support was provided by IBM and by NSF Presidential Young Investigator Awards PYIA 8351179 (E.W.K.) and CBT 8657444 (J.A.N.Z.) with matching funds from the Petroleum Research Fund, the Exxon Education Foundation, and the Du Pont Company.

12 May 1989; accepted 8 August 1989

Bacterial Blight of Soybean: Regulation of a Pathogen Gene Determining Host Cultivar Specificity

THANH V. HUYNH,* DOUGLAS DAHLBECK, BRIAN J. STASKAWICZ

Soybean cultivars resistant to *Pseudomonas syringae* pathovar *glycinea* (*Psg*), the causal agent of bacterial blight, exhibit a hypersensitive (necrosis) reaction (HR) to infection. *Psg* strains carrying the *avrB* gene elicit the HR in soybean cultivars carrying the resistance gene *Rpg1*. *Psg* expressing *avrB* at a high level and capable of eliciting the HR in the absence of de novo bacterial RNA synthesis have been obtained in in vitro culture. Nutritional signals and regions within the *Psg hrp* gene cluster, an approximately 20-kilobase genomic region also necessary for pathogenicity, control *avrB* transcription.

GENETIC STUDIES OF PLANT HOSTS and their parasites suggest that host resistance to disease requires specific pathogen recognition. Many interactions between particular host cultivars and particular natural variants ("races") of a pathogen culminate in disease resistance only when a specific avirulence gene in the pathogen and a resistance gene in the host are present (1). Interactions of this type are designated gene-for-gene host-parasite relationships.

Infection of soybean, *Glycine max* (L.) Merr., by *Pseudomonas syringae* pv. *glycinea* (*Psg*), the causal agent of bacterial blight, provides a model for investigating the molecular basis of a gene-for-gene interaction (2). *Psg* multiplies in the leaf intercellular fluid of susceptible soybean cultivars, where it induces the appearance of spreading, water-soaked, chlorotic lesions. In resistant soybean cultivars, the phenotype of disease resistance is typified by the hypersensitive reaction (HR): leaf mesophyll cells near the invading bacteria rapidly collapse to produce a desiccated necrotic lesion. In this reaction, bacterial multiplication is inhibited and the pathogen is localized at the site of

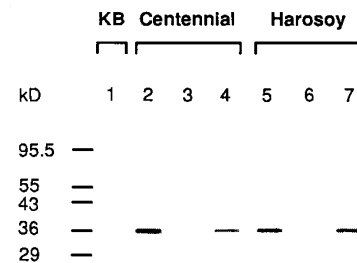
infection (3). Soybean cultivars carrying the dominant resistance gene *Rpg1* produce hypersensitive lesions when infected by *Psg* races carrying the avirulence gene *avrB* (2, 4). Thus, the interaction between *avrB* and *Rpg1* represents a gene-for-gene relation. Here we address the relation between *avrB* and other *Psg* genes required for the bacterium to elicit the HR.

Psg race 0 (*Psg*0), which contains *avrB*, is avirulent (that is, HR-inducing) on the *Rpg1*-containing soybean cultivar (cv.) Harosoy and virulent on cv. Centennial (2, 5).

The dark brown lesions characteristic of the *avrB-Rpg1* interaction begin to appear approximately 9 hours after inoculation of *Psg*0 into a Harosoy leaf. To detect *avrB* expression, we used antibodies to a portion of the 36-kD polypeptide encoded by the *avrB* open reading frame (ORF) (legend to Fig. 1) in immunoblot analysis (6) of total lysates of *Psg* isolated from infected soybean leaves. An ~36-kD protein in *Psg*0 isolated from leaves of either the susceptible soybean cv. Centennial (Fig. 1, lane 2) or the resistant cv. Harosoy (lane 5) was detected. The signal was not produced by *Psg*0 grown in standard rich broth, King's B (KB) medium (7) (Fig. 1, lane 1), or by a *Psg*0 strain in which the *avrB* gene had been inactivated by a Tn5 insertion (2) (lanes 3 and 6). When the plasmid pPg0-01-17 bearing the cloned *avrB* gene (Fig. 2) was introduced into the *avrB* mutant strain, the race-specific HR-inducing activity and the ability of the bacteria to produce the 36-kD protein were restored (Fig. 1, lanes 4 and 7).

The 36-kD *avrB* gene product can be detected in bacteria grown in planta but not in KB broth. Soybean leaf extracts added to bacteria growing in KB broth [which contains peptone, glycerol, potassium phosphate, and MgSO₄ (7)] failed to induce *avrB* (8). In contrast, manipulating the carbon source in a defined culture medium did affect transcription from the *avrB* promoter. Expression of a plasmid-borne translational fusion between the 5' end of the *avrB* gene and the *Escherichia coli lacZ* gene encoding β-galactosidase (Fig. 2) was measured in *Psg*0 grown in minimal medium (MM) containing one of 14 different carbon sources utilizable by *Psg*0. Depending on the carbon source, the level of β-galactosidase activity varied 89-fold (Fig. 3). Bacteria grown in the presence of fructose, sucrose, or mannitol showed the greatest β-galactosidase ac-

Fig. 1. Detection of *avrB* protein in *Psg*0 recovered from infected soybean leaves. *Psg*0 (lanes 1, 2, and 5), *Psg*0Rif^r *avrB*::Tn5 (lanes 3 and 6), and *Psg*0Rif^r*avrB*::Tn5 carrying pPg-0-01-17 (Fig. 2), a plasmid containing a functional cloned copy of *avrB* (lanes 4 and 7), were grown in KB broth or soybean cvs. Centennial or Harosoy. For growth in plants, *Psg* grown in KB medium were suspended in 10 mM MgSO₄ [~3 × 10⁸ colony-forming units (CFU) per milliliter], inoculated into 2- to 3-week-old soybean seedlings by vacuum infiltration, and the infected plants were incubated (16). Leaf intercellular fluid containing bacteria was harvested 15 to 48 hours after inoculation (17). Total bacterial proteins were separated on a 10% SDS-polyacrylamide gel (18), transferred to nitrocellulose (6), and challenged with antibodies to the *avrB* protein prepared as follows. Rabbit antibodies to a fusion protein consisting of the COOH-terminal 281 amino acids encoded by the 963-nucleotide *avrB* ORF (19) fused to the COOH-terminus of *E. coli* β-galactosidase (20) were affinity-purified to the fusion protein immobilized on nitrocellulose (21). Antibodies to the β-galactosidase portion of the fusion protein were removed by adsorption to an *E. coli* extract containing β-galactosidase. The remaining antibodies were used in immunoblot analysis at a dilution of 1:8000 relative to the original serum. Bound antibody was visualized by reaction with alkaline phosphatase-conjugated goat antibodies to rabbit immunoglobulin G (Promega Biotec).



Department of Plant Pathology, University of California, Berkeley, CA 94720.

*Present address: Department of Molecular Biology and Genetics, The Johns Hopkins University School of Medicine, Baltimore, MD 21205.